Inelastic Lifetimes of Hot Electrons in Real Metals

I. Campillo,[1] J. M. Pitarke,[1,4] A. Rubio,[2] E. Zarate,[3] and P. M. Echenique[3,4]
[1]*Materia Kondentsatuaren Fisika Saila, Zientzi Fakultatea, Euskal Herriko Unibertsitatea, 644 Posta kutxatila, 48080 Bilbo, Basque Country, Spain*
[2]*Departamento de Física Teórica, Universidad de Valladolid, 47011 Valladolid, Spain*
[3]*Materialen Fisika Saila, Kimika Fakultatea, Euskal Herriko Unibertsitatea, 1072 Posta kutxatila, 20080 Donostia, Basque Country, Spain*
[4]*Donostia International Physics Center (DIPC) and Centro Mixto CSIC-UPV/EHU, Spain*
(Received 27 January 1999)

We report a first-principles description of inelastic lifetimes of excited electrons in real Cu and Al, which we compute, within the *GW* approximation of many-body theory, from the knowledge of the self-energy of the excited quasiparticle. Our full band-structure calculations indicate that actual lifetimes are the result of a delicate balance between localization, density of states, screening, and Fermi-surface topology. A major contribution from *d* electrons participating in the screening of electron-electron interactions yields lifetimes of excited electrons in copper that are larger than those of electrons in a free-electron gas with the electron density equal to that of valence ($4s^1$) electrons. In aluminum, a simple metal with no *d* bands, splitting of the band structure over the Fermi level results in electron lifetimes that are smaller than those of electrons in a free-electron gas.

PACS numbers: 71.45.Gm, 78.47.+p

Electron dynamics in metals are well known to play an important role in a variety of physical and chemical phenomena, and low-energy excited electrons have been used as new probes of many-body decay mechanisms and chemical reactivity [1]. Recently, the advent of time-resolved two-photon photoemission (TR-2PPE) [2] has made it possible to provide direct measurements of the lifetime of these so-called hot electrons in copper [3–8], other noble and transition metals [9], ferromagnetic solids [10], and high T_c superconductors [11]. Also, ballistic electron emission spectroscopy (BEES) has shown to be capable of determining hot-electron relaxation times in solid materials [12].

An evaluation of the inelastic lifetime of excited electrons in the vicinity of the Fermi surface was first reported by Quinn and Ferrell [13], within a many-body free-electron description of the solid, showing that it is inversely proportional to the square of the energy of the quasiparticle measured with respect to the Fermi level. Since then, several free-electron calculations of electron-electron scattering rates have been performed, within the random-phase approximation (RPA) [14,15] and with inclusion of exchange and correlation effects [16,17]. Band-structure effects were discussed by Quinn [18] and Adler [19], and statistical approximations were applied by Tung *et al.* [20] and by Penn [21]. Nevertheless, there was no first-principles calculation of hot-electron lifetimes in real solids, and further theoretical work was needed for the interpretation of existing lifetime measurements and, in particular, to quantitatively account for the interplay between band structure and many-body effects on electron relaxation processes.

In this Letter we report results of a full *ab initio* evaluation of relaxation lifetimes of excited electrons in real solids. First, we expand the one-electron Bloch states in a plane-wave basis [22], and solve the Kohn-Sham equation of density-functional theory (DFT) [23] by invoking the local-density approximation (LDA) for exchange and correlation [24]. The electron-ion interaction is described by means of a nonlocal, norm-conserving ionic pseudopotential [25], and we use the one-electron Bloch states to evaluate the screened Coulomb interaction within a well-defined many-body framework, the RPA [26]. We finally evaluate the lifetime from the knowledge of the imaginary part of the electron self-energy of the excited quasiparticle, which we compute within the so-called GW approximation of many-body theory [27].

Let us consider an inhomogeneous electron system. The damping rate of an excited electron in the state $\phi_0(\mathbf{r})$ with energy E is obtained as (we use atomic units throughout, i.e., $e^2 = \hbar = m_e = 1$)

$$\tau^{-1} = -2 \int d\mathbf{r} \int d\mathbf{r}' \, \phi_0^*(\mathbf{r}) \, \mathrm{Im}\Sigma(\mathbf{r}, \mathbf{r}'; E) \phi_0(\mathbf{r}') , \tag{1}$$

where $\Sigma(\mathbf{r}, \mathbf{r}'; E)$ represents the electron self-energy. In the so-called GW approximation, only the first term of the expansion of the self-energy in the screened interaction is considered, and after replacing the Green function (G) by the zero order approximation (G^0), one finds

$$\mathrm{Im}\Sigma(\mathbf{r}, \mathbf{r}'; E) = \sum_f \phi_f^*(\mathbf{r}') \, \mathrm{Im}W(\mathbf{r}, \mathbf{r}'; \omega) \phi_f(\mathbf{r}) , \tag{2}$$

where $\omega = E - E_f$ represents the energy transfer, the sum is extended over a complete set of final states $\phi_f(\mathbf{r})$

 0031-9007/99/83(11)/2230(4)$15.00

with energy E_f ($E_F \leq E_f \leq E$), E_F is the Fermi energy, and $W(\mathbf{r}, \mathbf{r}'; \omega)$ is the screened Coulomb interaction:

$$W(\mathbf{r}, \mathbf{r}'; \omega) = \int d\mathbf{r}'' \, \epsilon^{-1}(\mathbf{r}, \mathbf{r}'', \omega) v(\mathbf{r}'' - \mathbf{r}') . \quad (3)$$

Here, $v(\mathbf{r} - \mathbf{r}')$ represents the bare Coulomb interaction, and $\epsilon^{-1}(\mathbf{r}, \mathbf{r}', \omega)$ is the inverse dielectric function of the solid, which we evaluate within RPA [28].

We introduce Fourier expansions appropriate for periodic crystals, and find

$$\tau^{-1} = \frac{1}{\pi^2} \sum_f \int_{\mathrm{BZ}} d\mathbf{q} \sum_{\mathbf{G}} \sum_{\mathbf{G}'} \frac{B^*_{0f}(\mathbf{q} + \mathbf{G}) B_{0f}(\mathbf{q} + \mathbf{G}')}{|\mathbf{q} + \mathbf{G}|^2} \times \mathrm{Im}[-\epsilon^{-1}_{\mathbf{G},\mathbf{G}'}(\mathbf{q}, \omega)] , \quad (4)$$

where

$$B_{0f}(\mathbf{q}) = \int d^3\mathbf{r} \, \phi^*_0(\mathbf{r}) e^{i\mathbf{q}\cdot\mathbf{r}} \phi_f(\mathbf{r}) , \quad (5)$$

and where $\epsilon^{-1}_{\mathbf{G},\mathbf{G}'}(\mathbf{q}, \omega)$ represent Fourier coefficients of the inverse dielectric function of the crystal. $\mathbf{G}$ and $\mathbf{G}'$ are reciprocal lattice vectors, and the integration over $\mathbf{q}$ is extended over the first Brillouin zone (BZ).

In particular, if couplings of the wave vector $\mathbf{q} + \mathbf{G}$ to wave vectors $\mathbf{q} + \mathbf{G}'$ with $\mathbf{G} \neq \mathbf{G}'$, i.e., the so-called crystalline local-field effects are neglected, one can write

$$\tau^{-1} = \frac{1}{\pi^2} \sum_f \int_{\mathrm{BZ}} d\mathbf{q} \times \sum_{\mathbf{G}} \frac{|B_{0f}(\mathbf{q} + \mathbf{G})|^2}{|\mathbf{q} + \mathbf{G}|^2} \frac{\mathrm{Im}[\epsilon_{\mathbf{G},\mathbf{G}}(\mathbf{q}, \omega)]}{|\epsilon_{\mathbf{G},\mathbf{G}}(\mathbf{q}, \omega)|^2} . \quad (6)$$

If all one-electron Bloch states entering both the matrix elements $B_{0f}(\mathbf{q} + \mathbf{G})$ and the dielectric function $\epsilon_{\mathbf{G},\mathbf{G}}(\mathbf{q}, \omega)$ are represented by plane waves, then Eq. (6) exactly coincides with the GW formula for the scattering rate of excited electrons in a free-electron gas (FEG), as obtained by Quinn and Ferrell [13] and by Ritchie [14]. In the case of electrons with energy very near the Fermi energy ($E \approx E_F$) the phase space available for real transitions is simply $E - E_F$, which yields the well-known $(E - E_F)^2$ scaling of the scattering rate. In the high-density limit ($r_s \ll 1$) [29], one finds [13]

$$\tau_{\mathrm{QF}} = 263 r_s^{-5/2} (E - E_F)^{-2} \mathrm{eV}^2 \, \mathrm{fs} . \quad (7)$$

The hot-electron decay in real solids depends on both the wave vector $\mathbf{k}$ and the band index n of the initial Bloch state $\phi_0(\mathbf{r}) = e^{i\mathbf{k}\cdot\mathbf{r}} u_{\mathbf{k},n}(\mathbf{r})$. We have evaluated hot-electron lifetimes along various directions of the wave vector [30], and have found that scattering rates of low-energy electrons are strongly directional dependent. Since measurements of hot-electron lifetimes have been reported as a function of energy, we here focus on the evaluation of $\tau^{-1}(E)$, which we obtain by averaging $\tau^{-1}(\mathbf{k}, n)$ over all wave vectors and bands lying in the irreducible element of the Brillouin zone (IBZ) with the same energy. The results presented below have been found to be well converged for all hot-electron energies under study ($E - E_F = 1.0$–3.5 eV), and they all have been performed with inclusion of conduction bands up to a maximum energy of $\sim$25 eV above the Fermi level. The sampling of the BZ required for the evaluation of both the dielectric matrix and the hot-electron decay rate of Eqs. (4) and (6) has been performed on $16 \times 16 \times 16$ Monkhorst-Pack meshes [31]. The sums in Eqs. (4) and (6) have been extended over 15$\mathbf{G}$ vectors of the reciprocal lattice, the magnitude of the maximum momentum transfer $\mathbf{q} + \mathbf{G}$ being well over the upper limit of $\sim 2q_F$ (q_F is the Fermi momentum).

Our *ab initio* calculation of the average lifetime $\tau(E)$ of hot electrons in Cu, as obtained from Eq. (4) with full inclusion of crystalline local-field effects, is presented in Fig. 1 by solid circles. The lifetime of hot electrons in a FEG with the electron density equal to that of valence ($4s^1$) electrons in copper ($r_s = 2.67$) is exhibited in the same figure, by a solid line. Both calculations have been carried out within one and the same many-body framework, the RPA; thus, the ratio between our

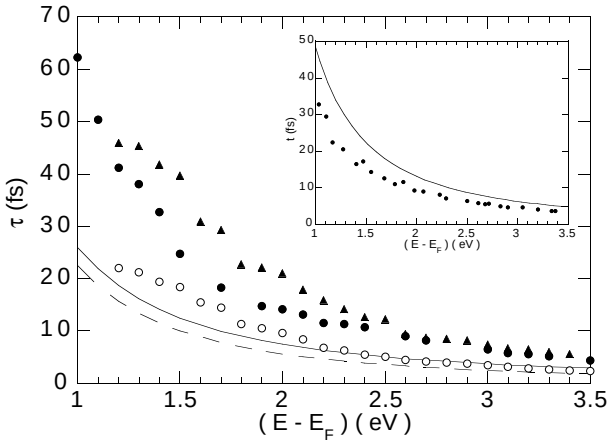

FIG. 1. Hot-electron lifetimes in Cu. Solid circles represent our full *ab initio* calculation of $\tau(E)$, as obtained after averaging $\tau(\mathbf{k}, n)$ of Eq. (4) over wave vectors and over the band structure for each $\mathbf{k}$. Solid and dashed lines represent the lifetime of hot electrons in a FEG with $r_s = 2.67$, as obtained within the full RPA (solid line) and from Eq. (7) (dashed line). Open circles represent the result obtained from Eq. (6) by replacing hot-electron initial and final states in $|B_{0f}(\mathbf{q} + \mathbf{G})|^2$ by plane waves and the dielectric function in $|\epsilon_{\mathbf{G},\mathbf{G}}(\mathbf{q}, \omega)|^{-2}$ by that of a FEG with $r_s = 2.67$, but with full inclusion of the band structure in the calculation of $\mathrm{Im}[\epsilon_{\mathbf{G},\mathbf{G}}(\mathbf{q}, \omega)]$. Full triangles represent the result obtained from Eq. (6) by replacing hot-electron initial and final states in $|B_{0f}(\mathbf{q} + \mathbf{G})|^2$ by plane waves, but with full inclusion of the band structure in the evaluation of both $\mathrm{Im}[\epsilon_{\mathbf{G},\mathbf{G}}(\mathbf{q}, \omega)]$ and $|\epsilon_{\mathbf{G},\mathbf{G}}(\mathbf{q}, \omega)|^{-2}$. The inset exhibits hot-electron lifetimes in Al. Solid circles represent our *ab initio* calculations, and the solid line represents lifetimes of hot electrons in a FEG with $r_s = 2.07$, as obtained within the full RPA.

calculated *ab initio* lifetimes and the corresponding FEG calculations unambiguously establishes the impact of the band structure of the crystal on the hot-electron decay. Our *ab initio* calculations indicate that the lifetime of hot electrons in copper is, within RPA, larger than that of electrons in a FEG with $r_s = 2.67$, this enhancement varying from a factor of ~ 2.5 near the Fermi level ($E - E_F = 1.0$ eV) to a factor of ~ 1.5 for $E - E_F = 3.5$ eV. We have also performed calculations of the lifetime of hot electrons in copper by just keeping the $4s^1$ Bloch states as valence electrons in the pseudopotential generation. The result of this calculation nearly coincides with the FEG calculations, showing the key role that d states play in the electron-decay mechanism.

First of all, we focus on the role that both localization and density of states (DOS) available for real excitations play in the hot-electron lifetime. Hence, we neglect crystalline local-field effects and evaluate hot-electron lifetimes from Eq. (6) by replacing the electron initial and final states in $|B_{0f}(\mathbf{q} + \mathbf{G})|^2$ by plane waves, and the dielectric function in $|\epsilon_{\mathbf{G},\mathbf{G}}(\mathbf{q}, \omega)|^{-2}$ by that of a FEG with $r_s = 2.67$. The result we obtain, with full inclusion of the band structure of the crystal in the evaluation of $\mathrm{Im}[\epsilon_{\mathbf{G},\mathbf{G}}(\mathbf{q}, \omega)]$, is represented in Fig. 1 by open circles. Since the states just below the Fermi level, which are available for real transitions, have a small but significant d component, they are more localized than pure sp states. Hence, their overlap with states over the Fermi level is smaller than in the case of free-electron states, and localization results in lifetimes of electrons with $E - E_F < 2$ eV that are slightly larger than predicted within the FEG model of the metal (solid line). At larger energies this band structure calculation predicts a lower lifetime than within the FEG model, due to opening of the d-band scattering channel dominating the DOS with energies from ~ 2.0 eV below the Fermi level.

While the excitation of d electrons diminishes the lifetime of electrons with energies $E - E_F > 2$ eV, d electrons also give rise to additional screening, thus increasing the lifetime of *all* electrons above the Fermi level. That this is the case is obvious from our band-structure calculation exhibited by full triangles in Fig. 1. This calculation is the result obtained from Eq. (6) by still replacing hot-electron initial and final states in $|B_{0f}(\mathbf{q} + \mathbf{G})|^2$ by plane waves (plane-wave calculation), but including the full band structure of the crystal in the evaluation of both $\mathrm{Im}[\epsilon_{\mathbf{G},\mathbf{G}}(\mathbf{q}, \omega)]$ and $|\epsilon_{\mathbf{G},\mathbf{G}}(\mathbf{q}, \omega)|^{-2}$. The effect of virtual interband transitions giving rise to additional screening is to increase, for the energies under study, the lifetime by a factor of ≈ 3, in qualitative agreement with the approximate prediction of Quinn [18].

Finally, we investigate band structure effects on hot-electron energies and wave functions. We have performed band-structure calculations of Eq. (4) with and without [see also Eq. (6)] the inclusion of crystalline local field corrections, and we have found that these corrections are negligible for $E - E_F > 1.5$ eV, while for energies very near the Fermi level, neglect of these corrections results in an overestimation of the lifetime of less than 5%. Therefore, differences between our full (solid circles) and plane-wave (solid triangles) calculations come from the sensitivity of hot-electron initial and final states on the band structure of the crystal. When the hot-electron energy is well above the Fermi level, these states are very nearly plane-wave states for most of the orientations of the wave vector, and the lifetime is well described by plane-wave calculations (solid circles and triangles nearly coincide for $E - E_F > 2.5$ eV). However, in the case of hot-electron energies near the Fermi level, initial and final states strongly depend on the orientation of the wave vector and on the shape of the Fermi surface. While the lifetime of hot electrons with the wave vector along the necks of the Fermi surface, in the ΓL direction, is found to be longer than the averaged lifetime by up to 80%, flattening of the Fermi surface along the ΓK direction is found to increase the hot-electron decay rate by up to 10% (see also Ref. [19]. Since for most orientations the Fermi surface is flattened, Fermi surface shape effects tend to decrease the average inelastic lifetime. An opposite behavior occurs for hole states with a strong d character below the Fermi level, localization of these states strongly increasing the hole lifetime [30].

Our band-structure calculation of hot-electron lifetimes in Al, as obtained from Eq. (4), is exhibited in the inset of Fig. 1 by solid circles, together with lifetimes of hot electrons in a FEG with $r_s = 2.07$ (solid line). Since aluminum is a simple metal with no d bands, $\mathrm{Im}[-\epsilon^{-1}_{\mathbf{G},\mathbf{G}'}(\mathbf{q}, \omega)]$ is well described within a free-electron model, and band structure effects enter only through the sensitivity of hot-electron initial and final wave functions on the band structure of the crystal. Because of splitting of the band structure over the Fermi level new decay channels are opened, and band structure effects now tend to decrease the hot-electron lifetime by a factor that varies from ~ 0.65 near the Fermi level ($E - E_F = 1$ eV) to a factor of ~ 0.75 for $E - E_F = 3$ eV.

Scaled lifetimes of hot electrons in Cu, as determined from most recent TR-2PPE experiments [5–7], are represented in Fig. 2, together with our calculated lifetimes of hot electrons in the real crystal (solid circles) and in a FEG with $r_s = 2.67$ either within the full RPA (solid line) or with use of Eq. (7) (dashed line). Though there are large discrepancies among results obtained in different laboratories, most experiments give lifetimes that are considerably longer than predicted within a free-electron description of the metal. At $E - E_F < 2$ eV, our calculations are close to lifetimes recently measured by Knoesel *et al.* in the very-low energy range [7]. At larger electron energies, good agreement between our band-structure calculations and experiment is obtained for

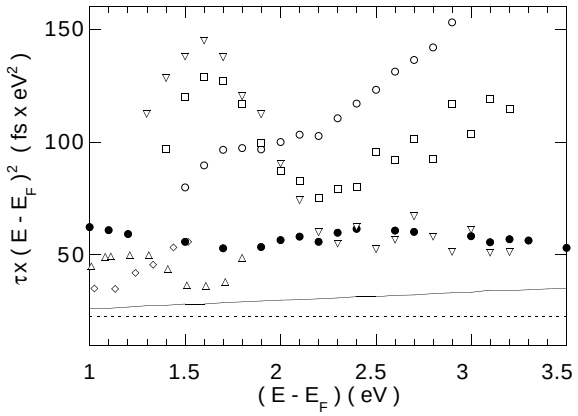

FIG. 2. Scaled lifetimes, $\tau \times (E - E_F)^2$, of hot electrons in Cu, as obtained from Eq. (4) with full inclusion of crystalline local-field effects (solid circles). Solid and dashed lines represent scaled lifetimes of hot electrons in a FEG with $r_s = 2.67$, as obtained within the full RPA (solid line) and from Eq. (7) (dashed line). Experimental lifetimes are taken from Ref. [5] (Cu[100]: squares; Cu[110]: inverted triangles; Cu[111]: open circles), from Ref. [6] with $\omega_{\text{photon}} = 1.63$ eV (diamonds), and from Ref. [7] (triangles).

Cu(110), where no band gap exists in the $\mathbf{k}_{\parallel} = 0$ direction. However, one must be cautious in the interpretation of TR-2PPE lifetime measurements, since they may be sensitive to electron transport away from the probed surface and also to the presence of the hole left behind in the photoexcitation process. In the case of injected electrons in BEES experiments no hole is present. A careful analysis of electron-electron mean free paths in these experiments [12] has shown a $(E - E_F)^{-2}$ dependence of hot-electron lifetimes in the noble metals, with an overall enhancement with respect to those predicted by Eq. (7) by a factor of ~ 2, in agreement with our band-structure calculations. We note that our calculated lifetimes (solid circles) approximately scale as $(E - E_F)^{-2}$, as a result of two competing effects. As the energy increases hot-electron lifetimes in a FEG (solid line) are known to be larger than those predicted by Eq. (7) (dashed line) [32], and this enhancement of the lifetime is nearly compensated by the reduction, at energies well over the Fermi level, of band structure effects.

In conclusion, we have performed full RPA band-structure calculations of hot-electron inelastic lifetimes in real solids, and have demonstrated that decay rates of excited electrons strongly depend on details of the electronic band structure. In the case of Cu, a subtle competition between localization, density of states, screening, and Fermi-surface topology results in hot-electron lifetimes that are larger than those of electrons in a FEG, and good agreement is obtained, for $E - E_F > 2$ eV, with observed lifetimes in Cu(110). For Al, interband transitions over the Fermi level yield hot-electron lifetimes that are smaller than those of electrons in a FEG.

We acknowledge partial support by the University of the Basque Country, the Basque Unibertsitate eta Ikerketa Saila, and the Spanish Ministerio de Educación y Cultura.

[1] H. Petek and S. Ogawa, Prog. Surf. Sci. **56**, 239 (1997).
[2] J. Bokor, Science **246**, 1130 (1989); R. Haight, Surf. Sci. Rep. **21**, 275 (1995).
[3] C. A. Schmuttenmaer *et al.*, Phys. Rev. B **50**, 8957 (1994).
[4] T. Hertel *et al.*, Phys. Rev. Lett. **76**, 535 (1996).
[5] S. Ogawa *et al.*, Phys. Rev. B **55**, 10 869 (1997).
[6] J. Cao *et al.*, Phys. Rev. B **56**, 1099 (1997).
[7] E. Knoesel *et al.*, Phys. Rev. B **57**, 12 812 (1998).
[8] A. Goldmann *et al.*, Surf. Sci. **414**, L932 (1998).
[9] E. Knoesel *et al.*, Surf. Sci. **368**, 76 (1996); J. Cao *et al.*, Phys. Rev. B **58**, 10 948 (1998).
[10] M. Aeschlimann *et al.*, Phys. Rev. Lett. **79**, 5158 (1997).
[11] W. Nessler *et al.*, Phys. Rev. Lett. **81**, 4480 (1998).
[12] K. Reuter *et al.*, Europhys. Lett. **45**, 181 (1999); K. Reuter *et al.* (to be published).
[13] J. J. Quinn and R. A. Ferrell, Phys. Rev. **112**, 812 (1958).
[14] R. H. Ritchie, Phys. Rev. **114**, 644 (1959)
[15] J. J. Quinn, Phys. Rev. **126**, 1453 (1962); J. C. Shelton, Surf. Sci. **44**, 305 (1974).
[16] R. H. Ritchie and J. C. Ashley, J. Phys. Chem. Solids **26**, 1689 (1963); L. Kleinman, Phys. Rev. B **3**, 2982 (1971); D. R. Penn, Phys. Rev. B **13**, 5248 (1976).
[17] D. R. Penn, Phys. Rev. B **22**, 2677 (1980).
[18] J. J. Quinn, Appl. Phys. Lett. **2**, 167 (1963).
[19] S. L. Adler, Phys. Rev. **130**, 1654 (1963).
[20] C. J. Tung *et al.*, Surf. Sci. **81**, 427 (1979).
[21] D. R. Penn, Phys. Rev. B **35**, 482 (1987).
[22] Kinetic-energy cutoffs of 75 and 12 Ry are introduced for Cu and Al, respectively. In the case of copper, all $4s^1$ and $3d^{10}$ Bloch states are kept as valence electrons in the pseudopotential generation.
[23] W. Kohn and L. Sham, Phys. Rev. **140**, A1133 (1965).
[24] D. M. Ceperley and B. J. Alder, Phys. Rev. Lett. **45**, 1196 (1980), as parametrized by J. P. Perdew and A. Zunger, Phys. Rev. B **23**, 5048 (1981).
[25] N. Troullier and J. L. Martins, Phys. Rev. B **43**, 1993 (1991).
[26] A. L. Fetter and J. D. Walecka, *Quantum Theory of Many-Particle Systems* (McGraw-Hill, New York, 1971).
[27] L. Hedin and S. Lundqvist, Solid State Phys. **23**, 1 (1969).
[28] A. A. Quong and A. G. Eguiluz, Phys. Rev. Lett. **70**, 3955 (1993); F. Aryasetiawan and K. Karlsson, Phys. Rev. Lett. **73**, 1679 (1994); N. E. Maddocks *et al.*, Europhys. Lett. **27**, 681 (1994); A. Fleszar *et al.*, Phys. Rev. Lett. **74**, 590 (1995); I. Campillo *et al.*, Phys. Rev. B **58**, 10 307 (1998).
[29] The so-called electron-density parameter r_s is defined by the relation $1/n_0 = (4/3)\pi(r_s a_0)^3$, n_0 being the average electron density, and a_0 the Bohr radius.
[30] I. Campillo, J. M. Pitarke, A. Rubio, and P. M. Echenique (to be published).
[31] H. J. Monkhorst and J. D. Pack, Phys. Rev. B **13**, 5188 (1976).
[32] P. M. Echenique, J. M. Pitarke, E. V. Chulkov, and A. Rubio, Chem. Phys. (to be published).